Electronic transmission through a polyacene ladder with a substitutional edge impurity

Malko Bravi,[1] Riccardo Farchioni,[2] Giuseppe Grosso,[2] and Giuseppe Pastori Parravicini[3]

[1]*Dipartimento di Fisica "A. Volta", Università di Pavia, Via A. Bassi, Pavia, Italy*

[2]*NEST-Istituto Nanoscienze of CNR and Dipartimento di Fisica "E. Fermi", Università di Pisa, Largo Pontecorvo 3, I-56127 Pisa, Italy*

[3]*Dipartimento di Fisica "A. Volta", Università di Pavia, Via A. Bassi, Pavia, Italy and Dipartimento di Fisica "E. Fermi", Università di Pisa, Largo Pontecorvo 3, I-56127 Pisa, Italy*

(Received 3 October 2012; published 4 January 2013)

We provide an analytical and numerical study of the electronic and transport properties of a ladder system composed of two coupled chains, arranged in the ladder polymer and in the polyacene lattice topology, with a single substitutional edge impurity embedded in one of them. We evidence in particular the connection between local density of states, transmittivity, and occurrence of Fano resonances in the transmission spectra. Comparison of the local density of states and charge transmittivity through the two different ladder systems, as the impurity position is varied, contributes to evidence the nature of resonant interactions occurring for electronic energies coinciding with the impurity energy.

DOI: 10.1103/PhysRevB.87.035105 PACS number(s): 72.10.Fk, 73.23.−b, 73.20.At

I. INTRODUCTION

Coherent transport in low-dimensional systems in the presence of constrictions, defects, disorder, and external fields has been widely addressed in the last decades (see Ref. 1 and references therein). In fact, such systems revealed a primary role in simulating and understanding quantum interference phenomena. One-dimensional and almost-one-dimensional quantum wire geometries have been generally adopted to describe electronic states and charge transport of a variety of systems which exhibit different structures, kinds of stochastic and correlated disorder, substitutional or side attached impurities, etc.[2–17] In particular, systems with parallel conduction paths have been fully exploited to study transmission conductance of electron wave guides, through single or multiple defects,[7–10] and to investigate the nature of Fano resonances or other quantum interference phenomena (see Ref. 18 and references therein), the nature of bound states degenerate with a continuum,[19,20] and also chain functionalization by side attached impurities.[21–24] Often, a tight-binding description of such systems in terms of appropriate site and hopping energies on a square net has proven to be very useful.[1,25]

In particular, this description can be convenient in molecular electronics, which is based on organic molecules, conjugated polymers, and graphene nanoribbons, a field which opened a very promising new avenue for technological applications. Differently from the ladder polymer case, however, mapping of organic materials on a model quantum wire system leads in general to a lattice with brick-type topology.[26] This is the case, for instance, of fused benzene rings as in acenes materials.[27] Polyacene, in particular, for its simplicity is at the center of numerous investigations, lasting for several decades,[28,29] as a prototype of conjugated polymers and also, more recently, as narrowest (two coupled chains) graphene ribbon (see, e.g., Refs. 30–32 and references therein). Most importantly, it has recently evidenced the potential of the presence of groups attached to molecular chains for the control of the position of the Fano resonances (see Ref. 33 and references therein). In particular, this can lead to significative modifications of the energy spectrum at the Fermi energy, with possible important influences on its thermoelectric and transport properties.[34]

In this paper, we revisit the problem of charge transport in two coupled parallel chains with geometrical arrangement compatible with the polyacene structure, and with a single substitutional impurity on one of them. Our approach exploits the tight-binding model with the decimation-renormalization procedure and the Green's function formalism for the electronic states and for the density of states.[35,36] By appropriate choice of the system parameters, our goal is to provide a recipe to tune the electronic structure of the ribbon, through chemical edge modification: this is an item central to nanotechnology for the control of the device behavior at the atomic scale. To reach such a goal, we show that coupling between chains in the presence of the edge impurity allows us to retain discrete states of the impurity resonant with continuum of the bands, at specific energies. At these energies, the transmittivity spectrum may change drastically showing Fano resonances, as in the case of a ladder polymer with a single substitutional impurity, but may also present isolated antiresonances; correspondingly, the electronic states may exhibit localized and propagating character of their wave functions,[20] with peculiar behavior of the projected density of states, the control of which is essential for understanding the system transmittivity.

In this article, we investigate and highlight the basic features of the electronic and transport properties of a two-chain ribbon, generated by the distinction that can be made in terms of topology between ladder polymer quantum wire and brick-type quantum wire. We show in particular that the topological peculiarity in the conformation of polyacene is at the origin of interesting novelties in the transport properties, with respect to the case of a ladder polymer topology, when edge substitutional impurities are present; these properties can be interpreted in a natural way by means of the deep differences induced by the lattice topology in the electronic properties.

In Sec. II, we present some main results concerning the case of a perfect two-coupled chains system with equal interchain and intrachain hopping interactions (ladder polymer) in the presence of a substitutional impurity on one chain; for it

we calculate the local density of states projected on different sites, and the system transmittivity. After decoupling the two chains into a symmetric and an antisymmetric channel, we show that the energy where the transmittivity of the active channel vanishes (due to the Fano resonance) coincides with a zero of the projection of the local density of states at the position of the impurity. The projection on the corresponding site of the adjacent channel presents a strong peak at a very close energy; also, this effect is due to the presence of the impurity.

In Sec. III, we deduce the expressions for the local density of states (LDOS) and the transmittivity of a polyacene chain both perfect and in the case of a substitutional impurity on one edge. We show that two inequivalent cases may occur, corresponding to the two inequivalent positions where the impurity can be located: on a site coupled or on a site uncoupled to the adjacent chain. We show moreover that the different electronic structure and in particular the opposite curvature of the bands in the negative and positive parts of the spectrum are relevant for the evaluation of the velocities of the charge carriers entering the expressions of the transmittivity on the two channels.

Section IV contains the results. We show that if the impurity is located on a site coupled to the adjacent chain, two Fano resonances are found in the transmission of one channel (depending on the attractive or repulsive nature of the impurity), which resemble the characteristic of the ladder polymer, while Fano resonances are absent in the other channel. If the impurity is located on a site uncoupled to the adjacent chain, a different behavior of the transmittivity is observed since in both channels an energy where the transmittivity vanishes exists, but just only one of them has the typical feature of a Fano resonance. Section V contains the conclusions.

II. EXPRESSIONS FOR THE LDOS AND THE TRANSMITTIVITY OF A LADDER POLYMER WITH A SINGLE SUBSTITUTIONAL EDGE IMPURITY

We consider the case of two coupled periodic chains with a substitutional impurity of energy a_d on the site $n = 0$ of one of them, a problem analyzed for instance in Refs. 7 and 8 [Fig. 1(a)]; we provide general expressions for this system which give information on the LDOS and the transmittivity. By an appropriate basis change,[7] we obtain two decoupled chains with site energies $a + t_\perp$ (symmetric combination S) and $a - t_\perp$ (antisymmetric combination A), respectively, and hopping intrachain interaction t [Fig. 1(b)]; the sites at $n = 0$ of the S and A chains have energies $a + t_\perp + a_d/2$ and $a - t_\perp + a_d/2$, respectively, and are coupled by an interaction of strength $a_d/2$. After resummation of the two semi-infinite left and right chains,[35] we obtain the equivalent system represented in Fig. 1(c). For the two sites of this system, the LDOS can be written in the forms ($t, t_\perp < 0$)

$$N_{0S}(E) = -\frac{1}{\pi}\mathrm{Im}\left(\frac{1}{E - \Sigma_S - \frac{(a_d/2)^2}{E-\Sigma_A}}\right) \times [2t + t_\perp \leqslant E \leqslant -2t + t_\perp], \quad (1)$$

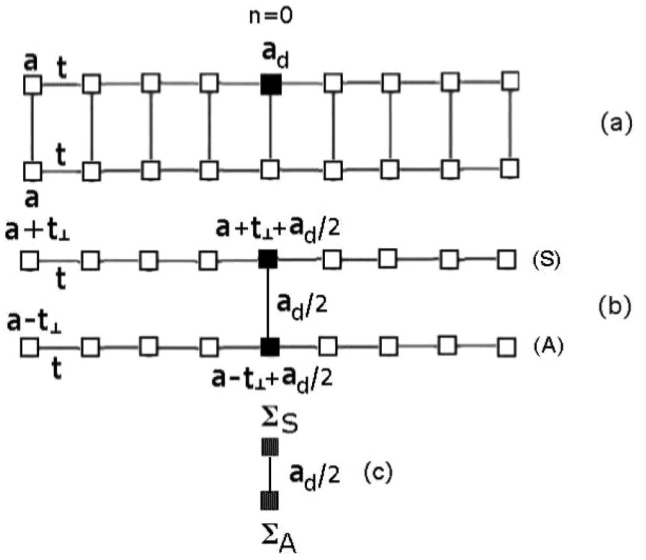

FIG. 1. (a) Two coupled identical chains of equal atoms with a substitutional impurity at the site $n = 0$ of one of them; (b) equivalent system formed by two decoupled (symmetric and antisymmetric) chains interacting only at the impurity position; (c) effective system obtained after renormalization of the semi-infinite periodic chains connected to the impurity.

$$N_{0A}(E) = -\frac{1}{\pi}\mathrm{Im}\left(\frac{1}{E - \Sigma_A - \frac{(a_d/2)^2}{E-\Sigma_S}}\right) \times [2t - t_\perp \leqslant E \leqslant -2t - t_\perp], \quad (2)$$

where ($a = 0$)

$$\Sigma_S = +t_\perp + a_d/2 + 2t^2 g_{00}(E; t_\perp, t), \quad (3)$$

$$\Sigma_A = -t_\perp + a_d/2 + 2t^2 g_{00}(E; -t_\perp, t), \quad (4)$$

and $g_{00}(E, \pm t_\perp, t)$ are the (0,0) matrix elements of the Green's functions of the semi-infinite periodic chains reported in Ref. 21 for the S and A chains, respectively. The effect of the impurity is to smooth the van Hove singularities of the LDOS present at the band borders of the perfect system spectrum. Moreover, the impurity may insert peaks which may be resonant with the allowed states of a single band, or isolated states outside the overall spectrum of the perfect system; these features are located at the right side of the allowed bands for $a_d > 0$ and at the left side for $a_d < 0$.

We evaluate now the transmittivity of the coupled chains with a substitutional impurity by exploiting the formalism of Conwell *et al.*[7] Let T_S and T_A be the transmittivities of electrons injected with wave vectors k_S and k_A, corresponding to the dispersion relations of the S and A chains, respectively. We introduce the real coefficients c_S^+, c_S^-, c_A^+, and c_A^- proportional to the velocity of electrons with wave vectors k_S and k_A on S and A bands, respectively:

$$c_S^\pm = t\sqrt{\pm\left[\left(\frac{E - t_\perp}{2t}\right)^2 - 1\right]}; \quad c_A^\pm = t\sqrt{\pm\left[\left(\frac{E + t_\perp}{2t}\right)^2 - 1\right]}. \quad (5)$$

In the intervals where only electrons with wave vector k_S or k_A propagate, the transmittivity of the system is $T = T_S = |t_{SS}|^2$ or $T = T_A = |t_{AA}|^2$ with

$$t_{SS[AA]} = \frac{2c_S c_A - c_{S[A]}(ia_d/2)}{2c_S c_A - (c_S + c_A)(ia_d/2)}, \tag{6}$$

where $c_S = c_S^-$ and $c_A = +ic_A^+$ when the channel S is active, $c_S = -ic_S^+$ and $c_A = c_A^-$ when the channel A is active. In the central energy intervals where electrons with both k_S and k_A propagate, $T = T_S + T_A$ where the transmittivities on the symmetric and the antisymmetric channels are

$$T_{S[A]} = \frac{c_{S[A]}^2\left(4c_{A[S]}^2 + a_d^2/4\right) + c_S c_A a_d^2/4}{4c_S^2 c_A^2 + (c_S + c_A)^2 a_d^2/4} \tag{7}$$

with $c_S = c_S^-$ and $c_A = c_A^-$. The conductance of the system can be evaluated accordingly by the two-probe Landauer formula $G = (2e^2/h)T$.

At the energies $E = 2t - t_\perp$ [where $c_A = 0$, see Eq. (5)] and $E = -2t + t_\perp$ [where $c_S = 0$, see Eq. (5)], respectively, i.e., at the borders of the central energy interval where both the channels of transmission are active, the symmetric and antisymmetric components of the transmittivity T_S and T_A are equal to one, independently from the value of a_d [see Eq. (6)]. Moreover, if $t < 0$, Fano resonances in the form of rapid variation of the transmittivity from 0 to 1 are observed, for T_S (T_A) when $a_d < 0$ ($a_d > 0$) (the reverse happens if $t > 0$). The energy where $T_S = 0$ (or $T_A = 0$) can be found by imposing $t_{SS} = 0$ (or $t_{AA} = 0$) in the form (6). For instance, the condition for $t_{AA} = 0$ is $2c_S = ia_d/2 = -2ic_S^+$, i.e., $a_d/2 = (-t/|t|)\sqrt{(E - t_\perp)^2 - 4t^2}$. This is illustrated by the plots of T_S and T_A reported in Fig. 2, where $t = t_\perp = -1$ and $a_d = 1$.

Looking at the corresponding plots of the LDOS projected on the impurity site, we can observe that, since $a_d > 0$, a strong peak in the LDOS is visible near the right border of the S band. Very close to a_d, there is a zero of the LDOS in the A band coincident with the zero of T_A: this originates the Fano feature in the transmittivity spectrum. The same happens for $a_d < 0$ on the left part of A and S spectra. The above considerations on the features of the LDOS and of the transmittivity provide a pictorial interpretation of the connection between the sign of the impurity site energy and the position of the Fano resonances in the transmission spectrum.

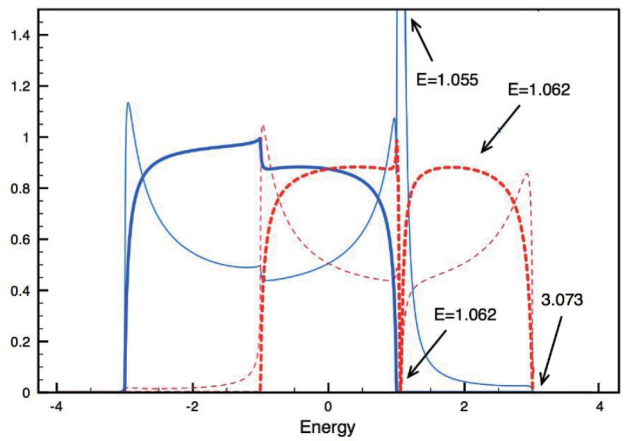

FIG. 2. (Color online) LDOS and transmittivity of the S channel (light and strong full blue lines, respectively) and A channel (light and strong dashed red lines, respectively) of two coupled chains ($a = 0$, $t = t_\perp = -1$) with a substitutional impurity of energy $a_d = 1$ on one of them; the LDOS is evaluated at the impurity site.

III. EXPRESSIONS FOR THE LDOS AND THE TRANSMITTIVITY OF POLYACENE WITH A SINGLE SUBSTITUTIONAL EDGE IMPURITY

A. Perfect polyacene chain

We address now the energy bands of a system composed by two coupled periodic atomic chains described by a tight-binding model with a single orbital per site, constant site energy a, first neighbor (negative) intrachain hopping interaction t, and (negative) interchain hopping interaction $t_\perp$ in the topology shown in Fig. 3, equivalent to the polyacene structure. Exploiting also in this case appropriate symmetric (S) and antisymmetric (A) linear combinations of the site orbitals of the two chains, it is possible to reduce the original ladder to an equivalent system composed by two decoupled chains with alternate site energies $a + t_\perp$ and a for the S chain, and $a - t_\perp$ and a for the A chain. Then, by renormalizing (for instance) the sublattice of the sites with energy a [hereafter named "noninteracting" because it is not coupled to the adjacent chain in the original system of Fig. 3(a); accordingly the sites with energies $a \pm t_\perp$ are named "interacting"], two periodic uncoupled chains are obtained with effective site energies $\tilde{a}_S(E) = a + t_\perp + 2t^2/(E - a)$, $\tilde{a}_A(E) = a - t_\perp + 2t^2/(E - a)$, and effective hopping interaction $\tilde{t} = t^2/(E - a)$ [see Fig. 3(d)].

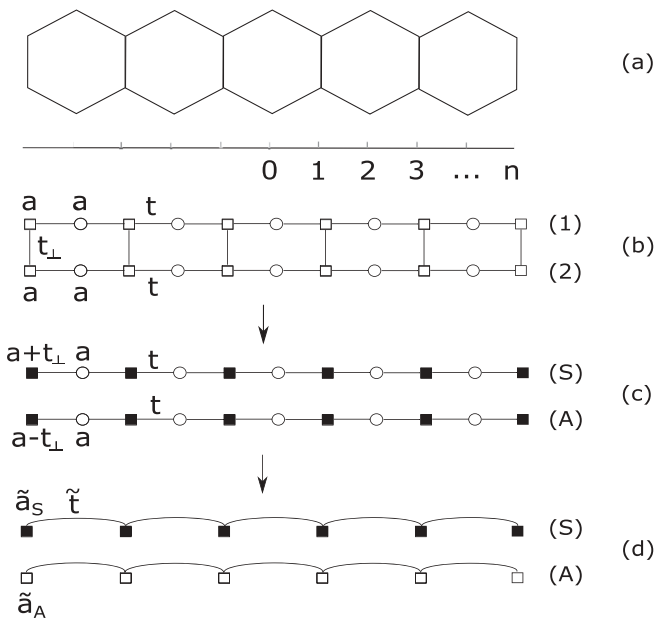

FIG. 3. (a) Polyacene chain; (b) chains coupled at alternate sites equivalent to the polyacene system; (c) decoupled symmetric and antisymmetric chains; (d) renormalized system for the calculation of the Green's function matrix elements.

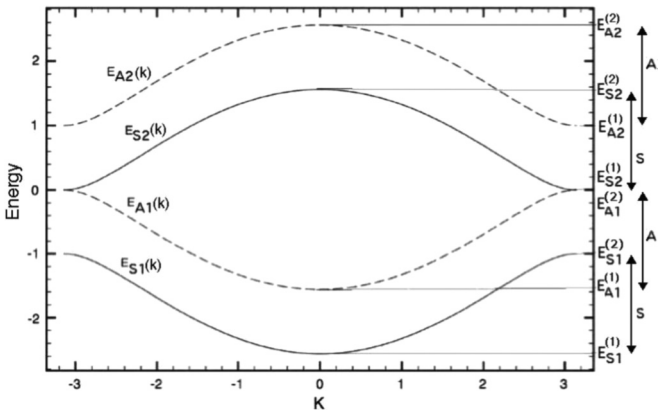

FIG. 4. Band structure of two chains coupled in the polyacene topology of Fig. 3(a), calculated for $a = 0$, $t = t_\perp = -1$. The edges of the bands $E_{S1}^{(1)} = -2.561$, $E_{S1}^{(2)} = -1$, $E_{S2}^{(1)} = 0$, $E_{S2}^{(2)} = 1.561$ for the S chain and $E_{A1}^{(1)} = -1.561$, $E_{A1}^{(2)} = 0$, $E_{A2}^{(1)} = 1$, $E_{A2}^{(2)} = 2.561$ for the A chain are evidenced.

The bands can then be extracted from the forms $E_{S,A}(k) = \tilde{a}_{S,A} \pm 2\tilde{t}\cos(k)$. Setting $a = 0$, from the equations $E_{S,A}(k) = \pm t_\perp + 2(t^2/E) + 2(t^2/E)\cos(k)$ we obtain the two couples of bands:

$$E_{S1,S2}(k) = \frac{t_\perp \pm \sqrt{t_\perp^2 + 8t^2(1+\cos(k))}}{2} \quad \text{(symmetric bands)}, \tag{8}$$

$$E_{A1,A2}(k) = \frac{-t_\perp \pm \sqrt{t_\perp^2 + 8t^2(1+\cos(k))}}{2} \quad \text{(antisymmetric bands)}, \tag{9}$$

which are reproduced in Fig. 4 for $a = 0$, $t = t_\perp = -1$. The energy extremals are $E_{S1}^{(1)} = (t_\perp - \sqrt{t_\perp^2 + 16t^2})/2$, $E_{A1}^{(1)} = (-t_\perp - \sqrt{t_\perp^2 + 16t^2})/2$, $E_{S1}^{(2)} = (t_\perp - |t_\perp|)/2$, $E_{A1}^{(2)} = E_{S2}^{(1)} = 0$, $E_{A2}^{(1)} = (-t_\perp + |t_\perp|)/2$, $E_{S2}^{(2)} = (t_\perp + \sqrt{t_\perp^2 + 16t^2})/2$, $E_{A2}^{(2)} = (-t_\perp + \sqrt{t_\perp^2 + 16t^2})/2$.

The LDOS projected on an interacting and a noninteracting site of the S and A chains can be evaluated by means of the imaginary part of the Green's function matrix elements reported in Appendices A and B, and are reproduced in Figs. 5(a) and 5(b). In Fig. 5(c), together with the band

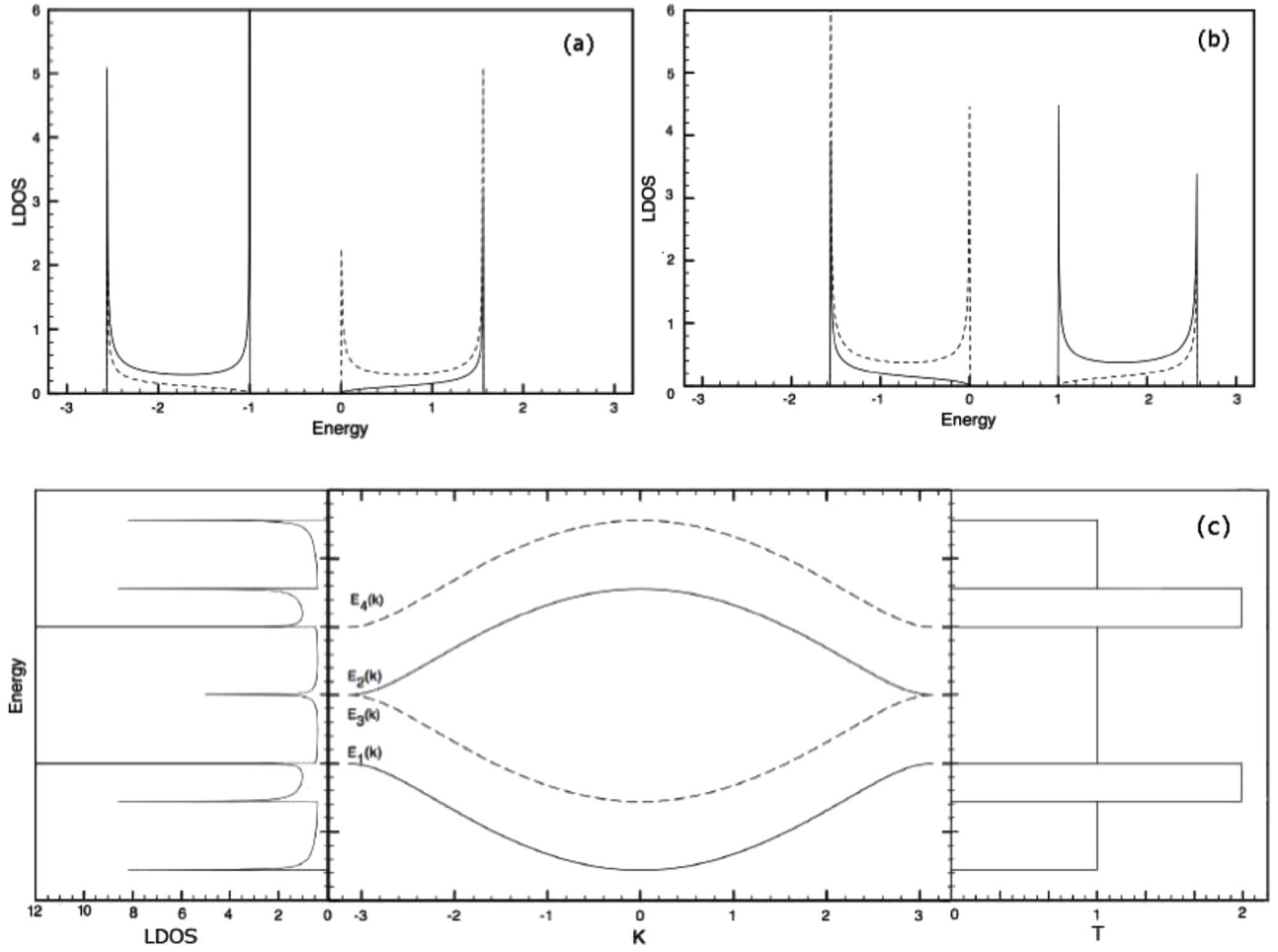

FIG. 5. LDOS of the perfect system projected on (a) an interacting (full lines) and a noninteracting site (dashed lines) of the symmetrical chain S; (b) an interacting (full lines) and a noninteracting site (dashed lines) of the antisymmetrical chain A; (c) on the left part is the sum of the LDOS on the two sites of the chains S and A, on the right is the total transmittivity as a function of the energy. The quantities are calculated for $a = 0$, $t = t_\perp = -1$.

structure, are reported the sum of the LDOS on the couple of sites of the two chains (on the left) and the transmittivity on the right. It can be observed that $T = 2$ in the energy intervals where S and A bands overlap and therefore the transmission can occur on both the corresponding channels, $T = 1$ in the energy intervals covered by a single S or A band, with the propagation occurring on the corresponding channel; $T = 0$ elsewhere.

B. Polyacene chain with a substitutional edge impurity

1. Local density of states

A substitutional impurity can be inserted into a polyacene chain in two nonequivalent positions, which correspond to the interacting or noninteracting sites of the system in Fig. 3(b). As for the problem of the coupled chains analyzed in the previous section, the chains can be decoupled into symmetrical (S) and antisymmetrical (A) parts, as shown in Figs. 6(a) and 6(b) for the two cases; after the decoupling, the impurities affect both chains at the same sites where they are located and are coupled by the interchain interaction $a_d/2$; the LDOS projected on relevant sites of the system can be then evaluated by suitable renormalizations and resummations of the S and A chains, as shown in Fig. 6.

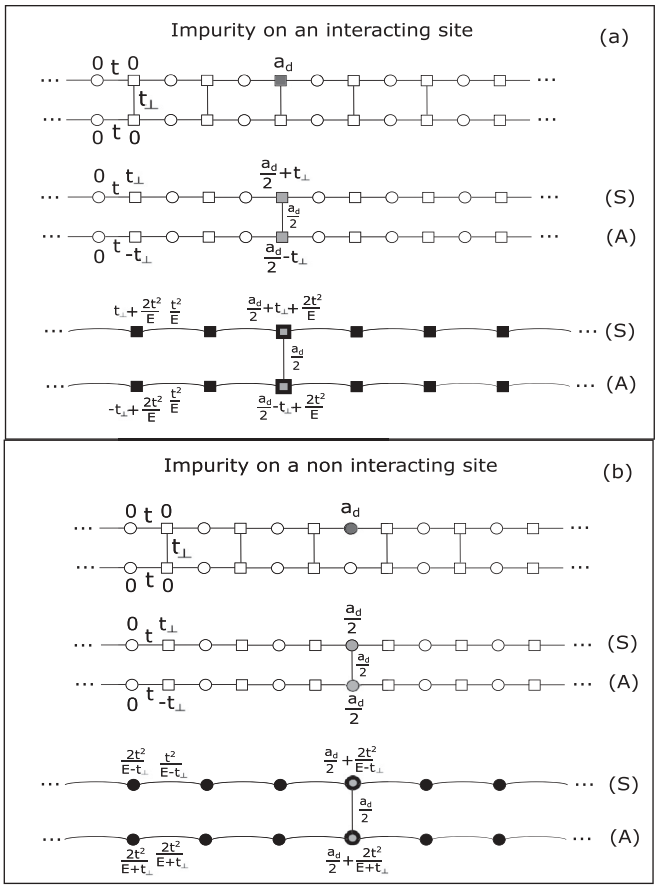

FIG. 6. Schematic procedure of the decoupling and renormalization for a polyacene chain with a substitutional impurity on (a) an interacting and (b) a noninteracting site.

2. Transmittivity

Exploiting the procedure adopted for the ladder polymer, we evaluate the transmittivity on the S and A channels of a polyacene chain with a substitutional impurity of site energy a_d. To calculate the coefficients c_S and c_A in the case of impurity located on an interacting or noninteracting site, we decouple and renormalize the system as in Figs. 6(a) and 6(b), respectively. The effective site energies and hopping interchain interactions for the impurity on the interacting site are

$$\tilde{a}_S = t_\perp + \frac{2t^2}{E}; \quad \tilde{a}_A = -t_\perp + \frac{2t^2}{E}; \quad \tilde{t}_S = \tilde{t}_A = \frac{t^2}{E}, \tag{10}$$

while for the impurity on the noninteracting site we have

$$\begin{aligned} \tilde{a}_S &= \frac{2t^2}{E - t_\perp}; \quad \tilde{t}_S = \frac{t^2}{E - t_\perp}; \\ \tilde{a}_A &= \frac{2t^2}{E + t_\perp}; \quad \tilde{t}_A = \frac{t^2}{E + t_\perp}. \end{aligned} \tag{11}$$

The above expressions can be inserted into the equations for the coefficients c_S and c_A, which in the case of polyacene are

$$c_S = i\tilde{t}_S \mathrm{sgn}(E)\sqrt{\left[\frac{E - \tilde{a}_S}{2\tilde{t}_S}\right]^2 - 1}, \tag{12}$$

$$c_A = -i\tilde{t}_A \mathrm{sgn}(E)\sqrt{\left[\frac{E - \tilde{a}_A}{2\tilde{t}_A}\right]^2 - 1}. \tag{13}$$

By substituting Eqs. (10) or (11) into the expressions for c_S and c_A, the transmittivity can then be evaluated by means of Eqs. (6) and (7).

IV. RESULTS FOR THE SUBSTITUTIONAL EDGE IMPURITY IN POLYACENE

A. Substitutional impurity on an interacting site

1. LDOS

In Fig. 7, we show the LDOS projected on the site where the impurity is located, for the S (full line) and A (dashed lines) chain, calculated for $t = t_\perp = -1$. As it can be noticed, for

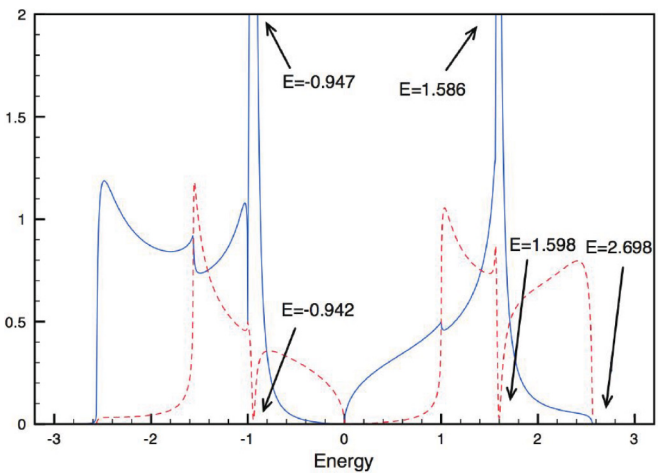

FIG. 7. (Color online) LDOS projected on an "interacting site" where the impurity is located for the S (blue full line) and A channels (red dashed lines) calculated for $t = t_\perp = -1$ and $a_d = 1$.

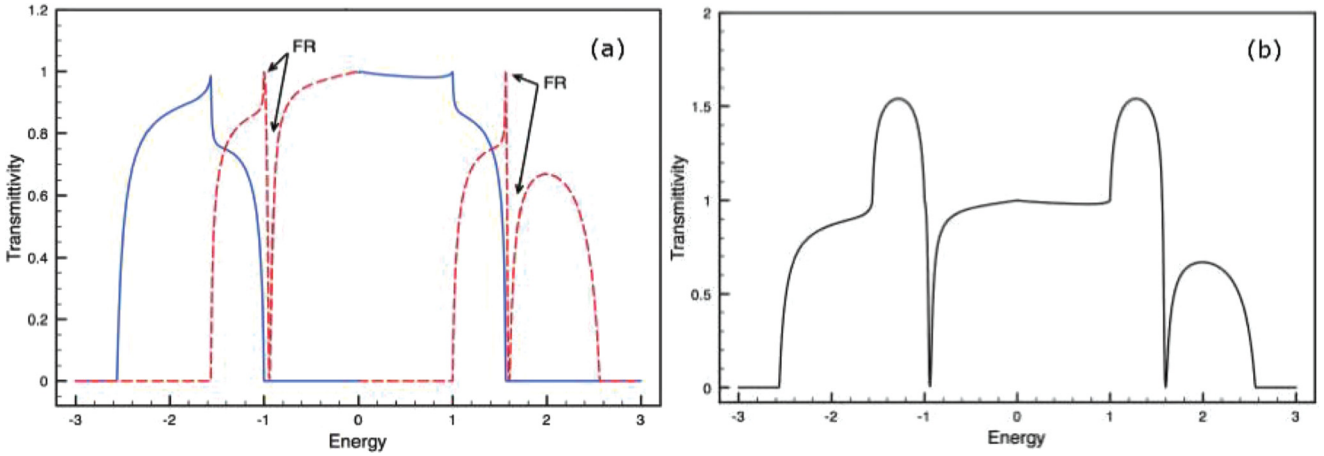

FIG. 8. (Color online) (a) Transmittivity of the S channel T_S (blue full line) and of the A channel T_A (red dashed line); (b) total transmittivity T of a polyacene chain with a substitutional impurity on an interacting site; $a_d = 1$, $t = t_\perp = -1$. The Fano resonances (FR) of T_A are indicated by arrows.

an impurity of positive energy ($a_d = 1$), two peaks are visible in the LDOS near the right borders of the two S bands of the perfect system. They occur at $E = -0.947$ and 1.586 which are internal to the continuum of the A bands, very close to dips at $E = -0.942$ and 1.598 where LDOS vanishes. A discrete state is present outside the spectrum of the perfect system, and is localized at $E = 2.698$.

The plot of T_S and T_A for a symmetrical incident wave calculated for $a_d = 1$ is reported in Fig. 8(a), and the total transmittivity T is reported in Fig. 8(b). As it can be noticed, the incident wave can propagate along the two channels and the impurity may also generate Fano resonances in the transmittivity. Let us analyze, for instance, the results for T_S. From Figs. 8(a) and 4, we realize that peaks with $T_S = 1$ are found at the onset of the two energy intervals where two channels of transmission are active [where $c_A = 0$, at $E = (-t_\perp - \sqrt{t_\perp^2 + 16t^2})/2 = -1.561$ and $E = -t_\perp$=1], as it happens also in the case of the ladder polymer of Sec. II.

An important novelty in the polyacene chain transmittivity is due to the fact that each channel presents two bands separated by a gap. For instance, in the case of the S channel, the gap extends between $E = E_{S1}^{(2)} = t_\perp$ to $E = E_{S2}^{(1)} = 0$ (see Fig. 4). If we approach this gap from below, i.e., for $E \lesssim E_{S1}^{(2)}$ where both c_S and c_A are real, we find that $c_S \to 0$ (and $c_A \to t^2/t_\perp$), and then T_S vanishes [see Eq. (7)]. Instead, approaching the gap from above, i.e., from $E \gtrsim E_{S2}^{(1)}$ where only the channel S is active (therefore c_S is real and c_A imaginary), we find that $c_S \to |t|\sqrt{t_\perp/E}$ and $c_A \to -i|t|\sqrt{t_\perp/E}$; these divergences lead to the result $T_S \to 1$ [see Eq. (6)], confirmed by the value of T_S reported in Fig. 8(a).

2. *Transmittivity*

Let us now investigate the conditions for Fano resonances in the polyacene chain, exploiting the expressions (12) and (13) of the coefficients c_S and c_A for the transmittivity; we remember that $T_S = 0$ if $2c_A - ia_d/2 = 0$, and $T_A = 0$ if $2c_S - ia_d/2 = 0$ [see Eq. (6)].[7] With respect to the case of the ladder polymer, for polyacene the S and A bands at $E > 0$ have opposite curvatures with respect to the bands at $E < 0$; this leads to opposite signs of the coefficients c_S and c_A, as specified in Eqs. (12) and (13). By combining these definitions with the conditions for the cancellation of T_S and T_A, one finds that for a positive value of the impurity energy ($a_d = 1$ in our case) no Fano resonance can be found for the S channel, while two Fano resonances exist in the transmittivity of the A channel, one for $E > 0$ and one for $E < 0$. The opposite happens if the impurity energy is negative. Due to the position of the impurity on an interacting site in the original chain, this result can be interpreted as a replica in the two bands of what is observed in the ladder polymer.

We remark that the energies of the dips in the Fano resonance where $T_A = 0$ coincide with the zeros of the LDOS in the same channel because they occur for conditions expressed by the same equation. For instance, in the case of Fig. 8(a), for $E < 0$ this happens at the solution of the condition $2c_S - ia_d/2 = 0$ (for vanishing T_A) and of the condition $2\sqrt{(E - t_\perp - 2t^2/E)^2 - (2t^2/E)^2} = a_d$ (for vanishing LDOS) which, after manipulations, can be shown to be the same equation. Similar considerations can be made for the Fano resonances occurring for the transmittivity of the S chain.

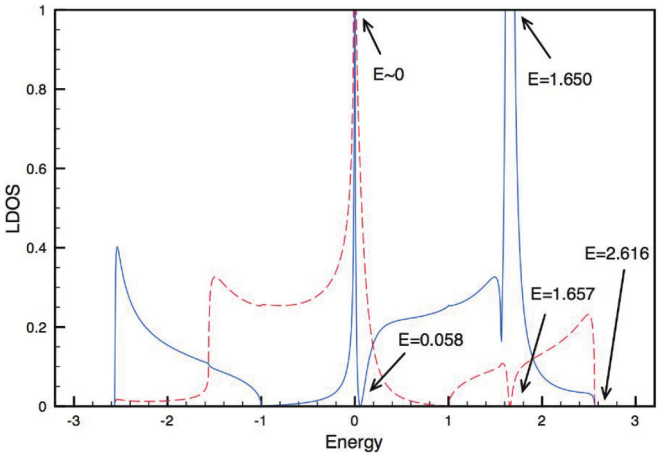

FIG. 9. (Color online) S (blue full line) and A (red dashed line) contributions to the LDOS projected on a "noninteracting site" where the impurity is located. $t = t_\perp = -1$, $a_d = 1$.

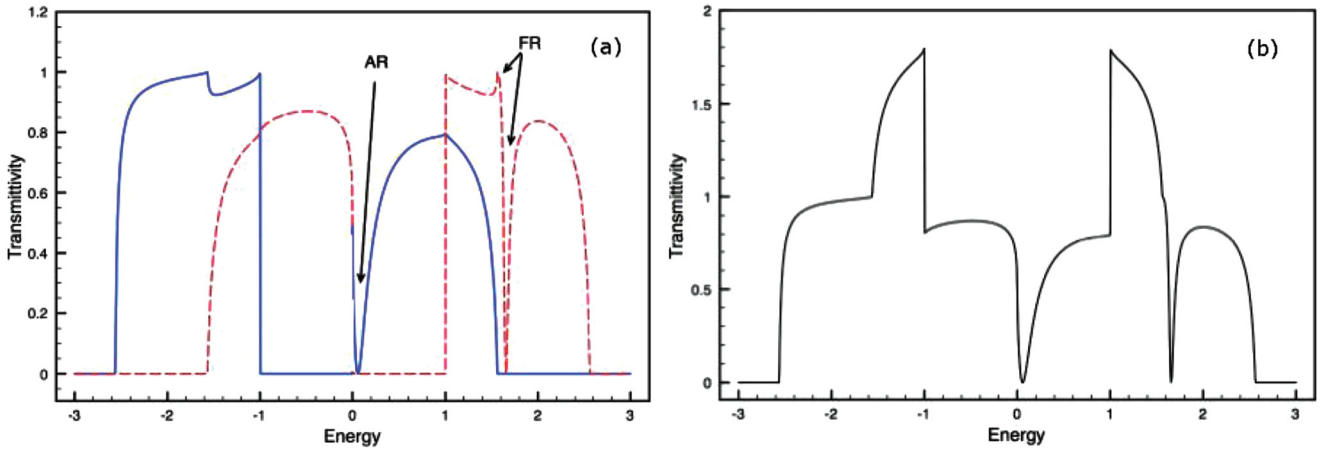

FIG. 10. (Color online) (a) Transmittivity of the S channel T_S (blue full line) and of the A channel T_A (red dashed line); (b) total transmittivity T of a polyacene chain with a substitutional impurity on a noninteracting site; $a_d = 1$, $t = t_\perp = -1$. The Fano resonance (FR) of T_A and the antiresonance (AR) of T_S are indicated by arrows.

B. Substitutional impurity on a noninteracting site

1. LDOS

In Fig. 9, we show the LDOS projected on the site of the primitive cell, where the impurity is located, which is not connected to the adjacent chain. It is worth to notice that this case is linked to the peculiar topology of the polyacene structure, and it is absent in the ladder polymer. A peak in the LDOS is observed at the right border of the higher-energy S band (at $E = 1.650$, internal to the spectrum of the perfect system) very near to a dip with zero minimum (at $E = 1.657$) in the LDOS evaluated at the site of the impurity in the A band. Moreover, another (very small) isolated peak external to the whole spectrum of the perfect system is found at $E = 2.616$.

Careful discussion must be paid to the peak in the LDOS at $E \sim 0$. In fact, it is made of the states at the right border of the lower energy A band and at the left border of the higher S band (see Fig. 4). The effect of the impurity is to merge these contributions resulting in the peak at $E \sim 0$ and in the dip at $E = 0.058$. Differently from the case of Fig. 7, we observe now that in Fig. 9 no peak occurs at the right border of the lower S band ($E \gtrsim -1$).

2. Transmittivity

The plots of T_S and T_A are reported in Fig. 10(a); let us analyze the behavior of T_S for specific energies. As it can be verified, $T_S = 1$ for $E = (-t_\perp - \sqrt{t_\perp^2 + 16t^2})/2$ [being $c_A = 0$, see Eq. (6)]; for $E \to t_\perp^-$, $c_S \to \sqrt{t^2/(E - t_\perp)}$, i.e., c_S diverges, leading again to the result that $T_S = 1$ [see Eq. (6)], just before the sharp drop to $T_S = 0$ at the onset of the energy gap; for $E \to 0^\pm$, both c_S and c_A approach zero: for instance, for $E \to 0^+$, $c_S \sim \sqrt{-t^2 E/t_\perp}$ and $c_A \sim -i\sqrt{-t^2 E/t_\perp}$. It follows that for $E \to 0^+$, $T_S \to 1/2$ (and $T_A = 0$) and similarly for $E \to 0^-$ $T_A \to 1/2$ (and $T_S = 0$).

For $E \to -t_\perp$, $c_A \to |tt_\perp|\sqrt{|t_\perp|}/\sqrt{E + t_\perp}$ and $|c_S| = 0.5$. Since we are at the border between one- and two-channel spectra, to estimate T_S we have to use the appropriate Eqs. (6) and (7) for $E \to -t_\perp^-$ and $E \to -t_\perp^+$, respectively. As a result, we find that at this energy $T_S = 1/[1 + (a_d^2/4)]$ (in our case $T_S = 0.8$ for $a_d = 1$); moreover, the energy dependence of T_S presents a different left and right derivative at $E = 1$ due to the difference between Eqs. (6) and (7) given by the term $c_s c_A a_d^2/4$.

Thus, differently from the case of impurity located on an interacting site, in the case of an impurity on a noninteracting site, only one "0-1" Fano resonance is observed. In fact, for the A channel a dip approaching zero in the transmittivity occurs for $E = 1.657$ (for $a_d = 1$) and the value $T_A = 1$ is at $E = 1.561$, which is the right border of the two-channel transmission [see arrow in Fig. 10(a)]. Instead, for the S channel only an antiresonance occurs at $E = 0.058$ (for $a_d = 1$), not associated to an energy value of complete transmittivity.

V. CONCLUSIONS

In this paper, we have studied the electronic and transport properties of a polyacene chain with a substitutional impurity on a single edge. We have addressed the effects of quantum coherence on the sample transmittivity and have shown how to connect intensity and position of the impurity to Fano resonances. We have adopted a tight-binding representation for the ladder system with polyacene topology, evaluating the density of states by the Green's function, and the transmittivity by the scattering matrix formalism.

We have found that if the impurity is located on a site interacting with the adjacent chain (as it happens in ordinary ladder polymer situations), two Fano resonances in the transmittivity are found: according to the sign of the impurity, these resonances are located in the symmetric or in the antisymmetric transmission channels. Conversely, we have observed that if the impurity is located on a site not interacting with the adjacent chain, only one Fano resonance is found in one transmission channel associated to an antiresonance in the transmission of the other channel. In all cases, a zero of the transmittivity in the symmetric or in the antisymmetric channel corresponds to a zero of the local density of states in the same channel projected on the site where the impurity is located, and to a peak at a close energy in the other channel.

APPENDIX A: GREEN'S FUNCTIONS AND LDOS OF PERFECT POLYACENE CHAINS: MATRIX ELEMENTS RELATIVE TO THE "INTERACTING" SITES

To obtain the Green's function matrix elements relative to a given sublattice of the chains S and A, we substitute the appropriate effective quantities $\tilde{a}_S$, $\tilde{a}_A$, and $\tilde{t}$ obtained by decimation of the other sublattice into the analytic forms for the infinite and semi-infinite periodic one-dimensional chain, respectively.[21] We can write the relevant energy intervals as

$$E-\tilde{a}\pm t_\perp > -2|\tilde{t}|,$$
$$E-\tilde{a}\pm t_\perp < +2|\tilde{t}|,$$
$$-2|\tilde{t}| < E-\tilde{a}\pm t_\perp < +2|\tilde{t}|,$$

where the minus sign before the interchain interaction corresponds to the S chain, and the plus sign to the A one. If we substitute the effective quantities obtained by the decimation of the sublattice with site energies 0 (noninteracting sites),

these intervals correspond to

$$[E-(2t^2/E)\pm t_\perp+(2t^2/|E|)]>0,\quad [E-(2t^2/E)\pm t_\perp-(2t^2/|E|)]<0,$$
$$[E-(2t^2/E)\pm t_\perp-(2t^2/|E|)]<0 \quad \text{and} \quad [E-(2t^2/E)\pm t_\perp+(2t^2/|E|)]>0.$$

We can then write the Green's function matrix elements relative to the "interacting" sites g^{∞}_{00S} in the form

$$g^{\infty}_{00S}=\begin{cases} -\frac{1}{\sqrt{\left(E-t_\perp-\frac{2t^2}{E}\right)^2-4\left(\frac{t^2}{E}\right)^2}} & \text{for} \quad E<\frac{t_\perp-\sqrt{t_\perp^2+16t^2}}{2}[E-\tilde{a}<-2|\tilde{t}|], \\ -\frac{i}{\sqrt{4\left(\frac{t^2}{E}\right)^2-\left(E-t_\perp-\frac{2t^2}{E}\right)^2}} & \text{for} \quad \frac{t_\perp-\sqrt{t_\perp^2+16t^2}}{2}<E<t_\perp[-2|\tilde{t}|<E-\tilde{a}<2|\tilde{t}|], \\ -\frac{1}{\sqrt{\left(E-t_\perp-\frac{2t^2}{E}\right)^2-4\left(\frac{t^2}{E}\right)^2}} & \text{for} \quad t_\perp<E<0[E-\tilde{a}<-2|\tilde{t}|], \\ -\frac{i}{\sqrt{4\left(\frac{t^2}{E}\right)^2-\left(E-t_\perp-\frac{2t^2}{E}\right)^2}} & \text{for} \quad 0<E<\frac{t_\perp+\sqrt{t_\perp^2+16t^2}}{2}[-2|\tilde{t}|<E-\tilde{a}<2|\tilde{t}|], \\ \frac{1}{\sqrt{\left(E-t_\perp-\frac{2t^2}{E}\right)^2-4\left(\frac{t^2}{E}\right)^2}} & \text{for} \quad E>\frac{t_\perp+\sqrt{t_\perp^2+16t^2}}{2}[E-\tilde{a}>2|\tilde{t}|]. \end{cases} \tag{A1}$$

The matrix elements g^{∞}_{00A} are

$$g^{\infty}_{00A}=\begin{cases} -\frac{1}{\sqrt{\left(E+t_\perp-\frac{2t^2}{E}\right)^2-4\left(\frac{t^2}{E}\right)^2}} & \text{for} \quad E<\frac{-t_\perp-\sqrt{t_\perp^2+16t^2}}{2}[E-\tilde{a}<-2|\tilde{t}|], \\ -\frac{i}{\sqrt{4\left(\frac{t^2}{E}\right)^2-\left(E+t_\perp-\frac{2t^2}{E}\right)^2}} & \text{for} \quad \frac{-t_\perp-\sqrt{t_\perp^2+16t^2}}{2}<E<-t_\perp[-2|\tilde{t}|<E-\tilde{a}<2|\tilde{t}|], \\ \frac{1}{\sqrt{\left(E+t_\perp-\frac{2t^2}{E}\right)^2-4\left(\frac{t^2}{E}\right)^2}} & \text{for} \quad -t_\perp<E<0[E-\tilde{a}>2|\tilde{t}|], \\ -\frac{i}{\sqrt{4\left(\frac{t^2}{E}\right)^2-\left(E+t_\perp-\frac{2t^2}{E}\right)^2}} & \text{for} \quad 0<E<\frac{-t_\perp+\sqrt{t_\perp^2+16t^2}}{2}[-2|\tilde{t}|<E-\tilde{a}<2|\tilde{t}|], \\ \frac{1}{\sqrt{\left(E+t_\perp-\frac{2t^2}{E}\right)^2-4\left(\frac{t^2}{E}\right)^2}} & \text{for} \quad E>\frac{-t_\perp+\sqrt{t_\perp^2+16t^2}}{2}[E-\tilde{a}>2|\tilde{t}|]. \end{cases} \tag{A2}$$

The analytic forms of the (0,0) matrix element for semi-infinite chains are

$$g_{00S}=\begin{cases} \frac{1}{2}\left(\frac{E}{t^2}\right)^2\left(E-t_\perp-\frac{2t^2}{E}+\sqrt{\left(E-t_\perp-\frac{2t^2}{E}\right)^2-4\left(\frac{t^2}{E}\right)^2}\right) & \text{for} \quad E<\frac{t_\perp-\sqrt{t_\perp^2+16t^2}}{2}[E-\tilde{a}<-2|\tilde{t}|], \\ \frac{1}{2}\left(\frac{E}{t^2}\right)^2\left(E-t_\perp-\frac{2t^2}{E}-i\sqrt{4\left(\frac{t^2}{E}\right)^2-\left(E-t_\perp-\frac{2t^2}{E}\right)^2}\right) & \text{for} \quad \frac{t_\perp-\sqrt{t_\perp^2+16t^2}}{2}<E<t_\perp[-2|\tilde{t}|<E-\tilde{a}<2|\tilde{t}|], \\ \frac{1}{2}\left(\frac{E}{t^2}\right)^2\left(E-t_\perp-\frac{2t^2}{E}+\sqrt{\left(E-t_\perp-\frac{2t^2}{E}\right)^2-4\left(\frac{t^2}{E}\right)^2}\right) & \text{for} \quad t_\perp<E<0[E-\tilde{a}<-2|\tilde{t}|], \\ \frac{1}{2}\left(\frac{E}{t^2}\right)^2\left(E-t_\perp-\frac{2t^2}{E}-i\sqrt{4\left(\frac{t^2}{E}\right)^2-\left(E-t_\perp-\frac{2t^2}{E}\right)^2}\right) & \text{for} \quad 0<E<\frac{t_\perp+\sqrt{t_\perp^2+16t^2}}{2}[-2|\tilde{t}|<E-\tilde{a}<2|\tilde{t}|], \\ \frac{1}{2}\left(\frac{E}{t^2}\right)^2\left(E-t_\perp-\frac{2t^2}{E}-\sqrt{\left(E-t_\perp-\frac{2t^2}{E}\right)^2-4\left(\frac{t^2}{E}\right)^2}\right) & \text{for} \quad E>\frac{t_\perp+\sqrt{t_\perp^2+16t^2}}{2}[E-\tilde{a}>2|\tilde{t}|] \end{cases} \tag{A3}$$

and

$$g_{00A}=\begin{cases}\frac{1}{2}\left(\frac{E}{t^2}\right)^2\left(E+t_\perp-\frac{2t^2}{E}+\sqrt{\left(E+t_\perp-\frac{2t^2}{E}\right)^2-4\left(\frac{t^2}{E}\right)^2}\right) & \text{for} \quad E<\frac{-t_\perp-\sqrt{-t_\perp^2+16t^2}}{2}[E-\tilde{a}<-2|\tilde{t}|],\\ \frac{1}{2}\left(\frac{E}{t^2}\right)^2\left(E+t_\perp-\frac{2t^2}{E}-i\sqrt{4\left(\frac{t^2}{E}\right)^2-\left(E+t_\perp-\frac{2t^2}{E}\right)^2}\right) & \text{for} \quad \frac{-t_\perp-\sqrt{t_\perp^2+16t^2}}{2}<E<0[-2|\tilde{t}|<E-\tilde{a}<2|\tilde{t}|],\\ \frac{1}{2}\left(\frac{E}{t^2}\right)^2\left(E+t_\perp-\frac{2t^2}{E}-\sqrt{\left(E+t_\perp-\frac{2t^2}{E}\right)^2-4\left(\frac{t^2}{E}\right)^2}\right) & \text{for} \quad 0<E<-t_\perp[E-\tilde{a}>2|\tilde{t}|],\\ \frac{1}{2}\left(\frac{E}{t^2}\right)^2\left(E+t_\perp-\frac{2t^2}{E}-i\sqrt{4\left(\frac{t^2}{E}\right)^2-\left(E+t_\perp-\frac{2t^2}{E}\right)^2}\right) & \text{for} \quad -t_\perp<E<\frac{-t_\perp+\sqrt{-t_\perp^2+16t^2}}{2}[-2|\tilde{t}|<E-\tilde{a}<2|\tilde{t}|],\\ \frac{1}{2}\left(\frac{E}{t^2}\right)^2\left(E+t_\perp-\frac{2t^2}{E}-\sqrt{\left(E+t_\perp-\frac{2t^2}{E}\right)^2-4\left(\frac{t^2}{E}\right)^2}\right) & \text{for} \quad E>\frac{-t_\perp+\sqrt{t_\perp^2+16t^2}}{2}[E-\tilde{a}>2|\tilde{t}|].\end{cases} \tag{A4}$$

APPENDIX B: GREEN'S FUNCTIONS AND LDOS OF PERFECT POLYACENE CHAIN MATRIX ELEMENTS ON THE "NONINTERACTING" SITES

By substituting the effective quantities obtained by the decimation of the sublattice of the interacting sites to the analytic forms, we obtain the Green's function matrix elements relative to the noninteracting sites in the form

$$g_{00S}^{\infty}=\begin{cases}-\frac{1}{\sqrt{\left(E-\frac{2t^2}{E-t_\perp}\right)^2-4\left(\frac{t^2}{E-t_\perp}\right)^2}} & \text{for} \quad E<\frac{t_\perp-\sqrt{t_\perp^2+16t^2}}{2},\\ -\frac{i}{\sqrt{4\left(\frac{t^2}{E-t_\perp}\right)^2-\left(E-\frac{2t^2}{E-t_\perp}\right)^2}} & \text{for} \quad \frac{t_\perp-\sqrt{t_\perp^2+16t^2}}{2}<E<t_\perp,\\ -\frac{1}{\sqrt{\left(E-\frac{2t^2}{E-t_\perp}\right)^2-4\left(\frac{t^2}{E-t_\perp}\right)^2}} & \text{for} \quad t_\perp<E<0,\\ -\frac{i}{\sqrt{4\left(\frac{t^2}{E-t_\perp}\right)^2-\left(E-\frac{2t^2}{E-t_\perp}\right)^2}} & \text{for} \quad 0<E<\frac{t_\perp+\sqrt{t_\perp^2+16t^2}}{2},\\ \frac{1}{\sqrt{\left(E-\frac{2t^2}{E-t_\perp}\right)^2-4\left(\frac{t^2}{E-t_\perp}\right)^2}} & \text{for} \quad E>\frac{t_\perp+\sqrt{t_\perp^2+16t^2}}{2},\end{cases} \tag{B1}$$

and the matrix elements g_{00A}^{∞} are

$$g_{00A}^{\infty}=\begin{cases}-\frac{1}{\sqrt{\left(E-\frac{2t^2}{E+t_\perp}\right)^2-4\left(\frac{t^2}{E+t_\perp}\right)^2}} & \text{for} \quad E<\frac{-t_\perp-\sqrt{t_\perp^2+16t^2}}{2},\\ -\frac{i}{\sqrt{4\left(\frac{t^2}{E+t_\perp}\right)^2-\left(E-\frac{2t^2}{E+t_\perp}\right)^2}} & \text{for} \quad \frac{-t_\perp-\sqrt{t_\perp^2+16t^2}}{2}<E<-t_\perp,\\ \frac{1}{\sqrt{\left(E-\frac{2t^2}{E}\right)^2-4\left(\frac{t^2}{E+t_\perp}\right)^2}} & \text{for} \quad -t_\perp<E<0,\\ -\frac{i}{\sqrt{4\left(\frac{t^2}{E+t_\perp}\right)^2-\left(E-\frac{2t^2}{E+t_\perp}\right)^2}} & \text{for} \quad 0<E<\frac{-t_\perp+\sqrt{t_\perp^2+16t^2}}{2},\\ \frac{1}{\sqrt{\left(E-\frac{2t^2}{E+t_\perp}\right)^2-4\left(\frac{t^2}{E+t_\perp}\right)^2}} & \text{for} \quad E>\frac{-t_\perp+\sqrt{t_\perp^2+16t^2}}{2}.\end{cases} \tag{B2}$$

The analytic forms of the (0,0) matrix element for semi-infinite chains are

$$g_{00S}=\begin{cases}\frac{1}{2}\left(\frac{E-t_\perp}{t^2}\right)^2\left(E-\frac{2t^2}{E-t_\perp}+\sqrt{\left(E-\frac{2t^2}{E-t_\perp}\right)^2-4\left(\frac{t^2}{E-t_\perp}\right)^2}\right) & \text{for} \quad E<\frac{t_\perp-\sqrt{t_\perp^2+16t^2}}{2}[E-\tilde{a}<-2|\tilde{t}|],\\ \frac{1}{2}\left(\frac{E-t_\perp}{t^2}\right)^2\left(E-\frac{2t^2}{E-t_\perp}-i\sqrt{4\left(\frac{t^2}{E-t_\perp}\right)^2-\left(E-\frac{2t^2}{E-t_\perp}\right)^2}\right) & \text{for} \quad \frac{t_\perp-\sqrt{t_\perp^2+16t^2}}{2}<E<t_\perp[-2|\tilde{t}|<E-\tilde{a}<2|\tilde{t}|],\\ \frac{1}{2}\left(\frac{E-t_\perp}{t^2}\right)^2\left(E-\frac{2t^2}{E-t_\perp}+\sqrt{\left(E-\frac{2t^2}{E-t_\perp}\right)^2-4\left(\frac{t^2}{E-t_\perp}\right)^2}\right) & \text{for} \quad t_\perp<E<0[E-\tilde{a}<-2|\tilde{t}|],\\ \frac{1}{2}\left(\frac{E-t_\perp}{t^2}\right)^2\left(E-\frac{2t^2}{E-t_\perp}-i\sqrt{4\left(\frac{t^2}{E-t_\perp}\right)^2-\left(E-\frac{2t^2}{E-t_\perp}\right)^2}\right) & \text{for} \quad 0<E<\frac{t_\perp+\sqrt{t_\perp^2+16t^2}}{2}[-2|\tilde{t}|<E-\tilde{a}<2|\tilde{t}|],\\ \frac{1}{2}\left(\frac{E-t_\perp}{t^2}\right)^2\left(E-\frac{2t^2}{E-t_\perp}-\sqrt{\left(E-\frac{2t^2}{E-t_\perp}\right)^2-4\left(\frac{t^2}{E-t_\perp}\right)^2}\right) & \text{for} \quad E>\frac{t_\perp+\sqrt{t_\perp^2+16t^2}}{2}[E-\tilde{a}>2|\tilde{t}|]\end{cases} \tag{B3}$$

and

$$g_{00A} = \begin{cases} \frac{1}{2}\left(\frac{E+t_\perp}{t^2}\right)^2\left(E - \frac{2t^2}{E+t_\perp} + \sqrt{\left(E - \frac{2t^2}{E+t_\perp}\right)^2 - 4\left(\frac{t^2}{E+t_\perp}\right)^2}\right) & \text{for} \quad E < \frac{-t_\perp - \sqrt{-t_\perp^2+16t^2}}{2}[E - \tilde{a} < -2|\tilde{t}|], \\ \frac{1}{2}\left(\frac{E+t_\perp}{t^2}\right)^2\left(E - \frac{2t^2}{E+t_\perp} - i\sqrt{4\left(\frac{t^2}{E+t_\perp}\right)^2 - \left(E - \frac{2t^2}{E+t_\perp}\right)^2}\right) & \text{for} \quad \frac{-t_\perp - \sqrt{t_\perp^2+16t^2}}{2} < E < 0[-2|\tilde{t}| < E - \tilde{a} < 2|\tilde{t}|], \\ \frac{1}{2}\left(\frac{E+t_\perp}{t^2}\right)^2\left(E - \frac{2t^2}{E+t_\perp} - \sqrt{\left(E - \frac{2t^2}{E+t_\perp}\right)^2 - 4\left(\frac{t^2}{E+t_\perp}\right)^2}\right) & \text{for} \quad 0 < E < -t_\perp[E - \tilde{a} > 2|\tilde{t}|], \\ \frac{1}{2}\left(\frac{E+t_\perp}{t^2}\right)^2\left(E - \frac{2t^2}{E+t_\perp} - i\sqrt{4\left(\frac{t^2}{E+t_\perp}\right)^2 - \left(E - \frac{2t^2}{E+t_\perp}\right)^2}\right) & \text{for} \quad -t_\perp < E < \frac{-t_\perp + \sqrt{-t_\perp^2+16t^2}}{2}[-2|\tilde{t}| < E - \tilde{a} < 2|\tilde{t}|], \\ \frac{1}{2}\left(\frac{E+t_\perp}{t^2}\right)^2\left(E - \frac{2t^2}{E+t_\perp} - \sqrt{\left(E - \frac{2t^2}{E+t_\perp}\right)^2 - 4\left(\frac{t^2}{E+t_\perp}\right)^2}\right) & \text{for} \quad E > \frac{-t_\perp + \sqrt{t_\perp^2+16t^2}}{2}[E - \tilde{a} > 2|\tilde{t}|]. \end{cases} \tag{B4}$$

[1] D. K. Ferry, S. M. Goodnick, and J. Bird, *Transport in Nanostructures* (Cambridge University Press, Cambridge, 2009).
[2] E. Tekman and P. F. Bagwell, Phys. Rev. B **48**, 2553 (1993).
[3] C. S. Kim, A. M. Satanin, Y. S. Joe, and R. M. Cosby, Phys. Rev. B **60**, 10962 (1999).
[4] A. M. Satanin and Y. S. Joe, Phys. Rev. B **71**, 205417 (2005).
[5] C. S. Kim and A. M. Satanin, Zh. Eksp. Teor. Fiz. **115**, 211 (1999) [J. Exp. Theor. Phys. **88**, 118 (1999)].
[6] P. F. Bagwell, Phys. Rev. B **41**, 10354 (1990).
[7] H. Mizes and E. Conwell, Phys. Rev. B **44**, 3963 (1991).
[8] C. Berthod, F. Gagel, and K. Maschke, Phys. Rev. B **50**, 18299 (1994).
[9] B. Y. Gu, C. R. Huo, Z. Z. Gan, G. Z. Yang, and J. Q. Wang, Phys. Rev. B **46**, 13274 (1992).
[10] I. Kander, Y. Imry, and U. Sivan, Phys. Rev. B **41**, 12941 (1990).
[11] Ch. Kunze, Phys. Rev. B **48**, 14338 (1993).
[12] J. U. Nockel and A. D. Stone, Phys. Rev. B **50**, 17415 (1994).
[13] V. Vargiamidis and V. Fessatidis, Phys. Rev. B **79**, 205309 (2009).
[14] W. Porod, Z. A. Shao, and C. S. Lent, Phys. Rev. B **48**, 8495 (1993).
[15] F. A. B. F. de Moura, R. A. Caetano, and M. L. Lyra, Phys. Rev. B **81**, 125104 (2010).
[16] A. Chakrabarti, Phys. Rev. B **74**, 205315 (2006).
[17] F. M. Izrailev, A. A. Krokhin, and N. M. Makarov, Phys. Rep. **512**, 125 (2012).
[18] A. Miroshnichenko, S. Flach, and Y. S. Kivshar, Rev. Mod. Phys. **62**, 2257 (2010).
[19] M. I. Molina, A. E. Miroshnichenko, and Y. S. Kivshar, Phys. Rev. Lett. **108**, 070401 (2012).
[20] V. Srivastava, Phys. Rev. B **41**, 5667 (1990).
[21] R. Farchioni, G. Grosso and G. P. Parravicini, Eur. Phys. J. B **84**, 227 (2011).
[22] R. Farchioni, G. Grosso and G. P. Parravicini, Phys. Rev. B **85**, 165115 (2012).
[23] H. Nakamura, N. Hatano, S. Garmon, and T. Petrosky, Phys. Rev. Lett. **99**, 210404 (2007).
[24] S. Garmon, H. Nakamura, N. Hatano, and T. Petrosky, Phys. Rev. B **80**, 115318 (2009).
[25] S. Datta, *Electronic Transport in Mesoscopic Systems*, Cambridge Studies in Semiconductor Physics and Microelectronic Engineering (Cambridge University Press, Cambridge, 1997).
[26] K. Wakabayashi, M. Fujita, H. Ajiki, and M. Sigrist, Phys. Rev. B **59**, 8271 (1999).
[27] M. Ezawa, Phys. Rev. B **73**, 045432 (2006).
[28] S. Kivelson and O. L. Chapman, Phys. Rev. B **28**, 7236 (1983).
[29] A. L. S. da Rosa and C. P. de Melo, Phys. Rev. B **38**, 5430 (1988).
[30] N. M. R. Peres and F. Sols, J. Phys.: Condens. Matter **20**, 255207 (2008).
[31] A. Cresti, G. Grosso and G. P. Parravicini, Phys. Rev. B **78**, 115433 (2008).
[32] L. Malysheva and A. Onipko, Phys. Rev. Lett. **100**, 186806 (2008).
[33] T. A. Papadopoulos, I. M. Grace, and C. J. Lambert, Phys. Rev. B **74**, 193306 (2006).
[34] D. Volja, B. Kozinsky, A. Li, D. Wee, N. Marzari, and M. Fornari, Phys. Rev. B **85**, 245211 (2012).
[35] G. Grosso and G. Pastori Parravicini, *Solid State Physics* (Academic, San Diego, 2000).
[36] E. N. Economou, *Green's Functions in Quantum Physics* (Springer, Berlin, 2006).